

Singlet oxygen quantum yields of potential porphyrin-based photosensitisers for photodynamic therapy†

Sean Mathai, Trevor A. Smith and Kenneth P. Ghiggino*

Received 18th April 2007, Accepted 25th July 2007

First published as an Advance Article on the web 31st July 2007

DOI: 10.1039/b705853e

The singlet oxygen formation quantum yield (Φ_{Δ}) for solutions of the di-cation, free-base and metallated forms of hematoporphyrin derivative (HpD), hematoporphyrin IX (Hp9) and a boronated protoporphyrin (BOPP) are reported using the method of direct detection of the characteristic phosphorescence following polychromatic excitation. Values of Φ_{Δ} for the free-base form of all the porphyrins and the di-cation forms of Hp9 and HpD are in the range of 0.44 to 0.85 in the solvents investigated. Incorporation of zinc ions into the macrocycle reduces Φ_{Δ} for all three porphyrins. BOPP facilitates the coordination of certain transition metals (Mn, Co and Cu) compared to Hp9 and HpD and results in a dramatic decrease in Φ_{Δ} . The experimental data suggest the introduction of low energy charge transfer states associated with the disruption of the planarity of the macrocyclic ring provides alternative non-radiative deactivation pathways. In BOPP, this non-planarity is augmented by the large *closo*-carborane peripheral substituent groups.

Introduction

Oxygen plays an important role in a wide variety of photochemical processes. The presence of unpaired valence electrons in the ground state configuration of molecular oxygen is unusual and confers a high chemical reactivity.¹ The atypical electron configuration of molecular oxygen gives rise to three energetically close lying electronic states; the Σ triplet ground state, and the excited Δ and Σ singlet states.^{2–4} The three lowest lying states of molecular oxygen are given the group theoretical and leading symbols $X^3\Sigma_g^-$, $a^1\Delta_g$ and $b^1\Sigma_g^+$ for the ground and first excited states. Any of the transitions between the ground state X and either of the lowest lying excited states would be a g–g transition and therefore forbidden according to parity selection rules. Further restrictions are also imposed for a singlet \leftrightarrow triplet and $\Sigma \leftrightarrow \Delta$ transitions.⁵ Therefore both the lowest lying excited states are termed metastable.^{6,7}

Singlet oxygen can be produced by chemical reaction,⁸ gas phase discharge⁹ or a photosensitisation reaction with the latter method being the most common.¹⁰ Once produced singlet oxygen can relax by radiative, non-radiative or quenching processes. The emission spectroscopic method,^{11–14} calorimetric methods, (in particular laser-induced opto-acoustic calorimetry),^{14–16} time resolved thermal lensing,^{17–19} and chemical quenching experiments^{16,20,21} have been used for monitoring singlet oxygen formation. Large discrepancies in the reported values of singlet oxygen quantum yields have been attributed to the differing methods used for determining this value.^{22,23} It is widely considered that direct observation of singlet oxygen emission in the IR region of the spectrum provides the most accurate determination of singlet

oxygen quantum yields.^{21,24,25} Advances in IR detectors have provided impetus for the more widespread application of the singlet oxygen phosphorescence method.^{26–28}

Singlet oxygen has been implicated as an intermediary species leading to cell death following photoexcitation of sensitising agents in the photodynamic therapy (PDT) of tumours.^{29–32} Measurements of singlet oxygen yields are thus important in assessing the potential effectiveness of photosensitising agents for PDT. In this study a slightly modified version of the singlet oxygen phosphorescence method has been used to determine the singlet oxygen formation quantum yields for various forms of three porphyrins suggested for use as sensitisers in PDT. The influence of solvent, solution pH and metallation of the porphyrins on singlet oxygen yields are a particular focus of the investigation.

Materials and methods

Chemicals

Hematoporphyrin IX dihydrochloride (Hp9, Porphyrin Products), hematoporphyrin derivative (HpD, Porphyrin Products), the tetrakis(carborane) carboxylate ester of 2,4-(α,β -dihydroxyethyl)deuterioporphyrin IX (BOPP, synthesised as described previously³³ and provided by S. Styli, Royal Melbourne Hospital) and Rose Bengal (RB, ABN Chemicals) were all used as received. Methanol (ICN Biomedicals Inc.), ethanol (Merck), acetone (Ajax Fine Chemicals) and acetonitrile (BDH) were of spectroscopic grade and used as supplied.

Accurate weights of the photosensitiser were obtained with an electromagnetic ultramicrobalance (Perkin-Elmer Auto-balance AM-2). An anti-static gun (Aldrich Zerostat 3) was used to eliminate static charge build up on the balance pans that would lead to erroneous recorded weights. Stock solutions (10^{-3} M) of the solute of interest were prepared in volumetric flasks and subsequently diluted to achieve sample concentrations in the range of 10^{-6} – 10^{-5} M.

School of Chemistry, The University of Melbourne, VIC, 3010, Australia.
E-mail: ghiggino@unimelb.edu.au; Fax: +61 3 9347 5180; Tel: +61 3 8344 7137

† This paper was published as part of the special issue in honour of David Phillips.

pH studies allowed investigation of the di-cation, di-anion and the free-base (Fb) forms of the porphyrins. Aqueous hydrochloric acid or sodium hydroxide solutions were added as required to achieve the desired degree of porphyrin protonation. Buffer solutions, known to interfere with the singlet oxygen production leading to lower observable quantum yields, were avoided in the current study.³⁴

Manganese(II) sulfate (MnSO_4 , BDH), iron(II) sulfate (FeSO_4 , BDH), zinc(II) sulfate (ZnSO_4 , BDH) and cobalt(II) chloride (CoCl_2), nickel(II) sulfate (NiSO_4) and copper(II) nitrate ($\text{Cu}(\text{NO}_3)_2$) (all provided by S. Boyd, University of Melbourne) were used for the metal complexation experiments. Metal complexes of the porphyrins were prepared by adding approximately 25 μL of concentrated aqueous solutions of the metal salt to the free-base porphyrin samples. These were then allowed to stand in the dark for approximately 48–72 h to ensure complete complexation. Addition of a small volume of aqueous NaOH was found to encourage the metallation process in the acetone and acetonitrile samples. Control experiments conducted with similar aqueous additions but without metal salts did not significantly affect singlet oxygen yields in the porphyrin solutions, confirming that the small amounts of water were not influencing the results.

Steady-state experiments

Steady-state absorption spectra were recorded on a Varian Cary Bio50 UV-Vis absorption spectrophotometer. Spectra were recorded against solvent blanks in matched 1 cm pathlength quartz cells. Cuvettes were acid washed and rinsed copiously with Milli-Q deionized water then dried in an oven at 120 °C prior to use. Photostability of the samples was monitored by recording absorption spectra before and after irradiation experiments.

Steady state fluorescence emission and excitation spectra were collected on a Cary Eclipse fluorescence spectrophotometer with excitation and emission bandwidths of 5 nm. Solutions were prepared to have an absorbance of approximately 0.1 at the excitation wavelength to minimize inner-filter effects.

Singlet oxygen quantum yield determinations

Fig. 1 shows a schematic diagram of the experimental arrangement used for the singlet oxygen quantum yield determinations. A white light xenon arc lamp (PoliLight, Rofin, Australia, model PL6) was employed as the excitation source providing a convenient, broad excitation wavelength range *via* light pipe delivery. Suitable filtering of the lamp output allowed selective excitation into different spectral regions. A heat filter, (KG3, Schott) blocked stray infrared (IR) or ultra-violet (UV) light whilst allowing simultaneous excitation into the Soret and Q-band regions. Further selectivity of the PoliLight output was achieved with the addition of a long pass filter (GG435 or GG495, Schott) to provide specific excitation into the different Q-bands whilst preventing excitation into the Soret band. The appropriately filtered spectral output from the light pipe was recorded using a fibre optic spectrometer (Ocean Optics Inc.). Calibration of the spectral response of the spectrometer over the 300–900 nm spectral range was achieved using a Calibrated Tungsten Halogen Light Source (LS-1-CAL, Ocean Optics Inc.) allowing the measurements using the various filtered outputs of the PoliLight to be corrected accordingly.

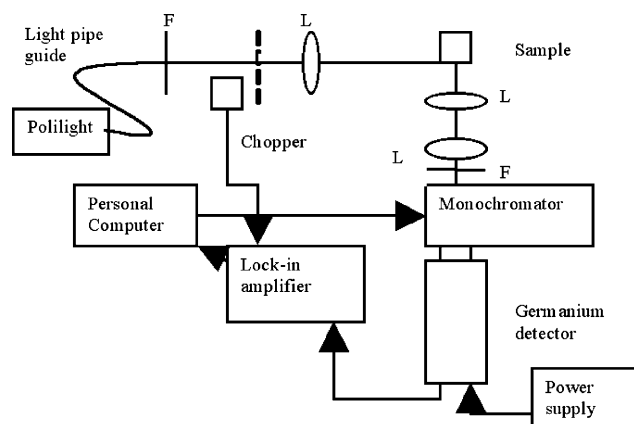


Fig. 1 Schematic of the experimental arrangement for the measurement of singlet oxygen emission and quantum yields: L-focussing lens; F-filter. Arrowed lines represent electrical connections.

The excitation light path was perpendicular to the detection path with the excitation beam weakly focussed using a 50 cm focal length convex lens to illuminate the front face of the sample cell, as depicted in Fig. 1, in order to minimise re-absorption of the singlet oxygen phosphorescence signal by the solvent. A homemade sample holder allowed reproducible sample positioning and minimised scattered light. Further elimination of stray light was achieved through the use of an iris in front of the PoliLight output. Solvent blanks were used to determine the presence of solvent fluorescence or other background signals that may interfere with the singlet oxygen phosphorescence. There was negligible IR emission from the quartz cells, solvents or optical components used in the experimental arrangement.

The NIR emission was collected at right angles to the excitation path, collimated, and focussed onto the entrance slit of a dual port/triple grating monochromator/spectrograph (Acton Research Corporation, SpectraPro 300i). The grating used was ruled at 300 grooves mm^{-1} and blazed at 1 μm . An IR-sensitive liquid nitrogen cooled germanium diode detector and amplifier (Applied Detector Corporation, model 403 L) biased at -180 V was used. The detector has a large active area of 25 mm^2 , a responsivity of $7 \times 10^9\text{ V W}^{-1}$ and a broad spectral response from 800–1700 nm.²⁶ In order to maximise detection sensitivity, the PoliLight output was modulated by an optical chopper (model 220A, HMS) and the modulated signal recorded by the germanium detector was sent to a lock-in amplifier (EG&G, model 5206, Princeton Applied Research) referenced to the chosen chopper frequency of 130 Hz.

A NIR filter (1185 LP, Omega Optical) was placed before the entrance slit of the monochromator in order to block any emission below 1200 nm. The singlet oxygen phosphorescence spectrum was collected by scanning the emission monochromator driven by a PC running a Visual Basic program, or the spectrograph was set to the maximum emission wavelength (1278 nm) of the singlet oxygen phosphorescence, and the intensities manually recorded from the digital display on the lock-in amplifier. The singlet oxygen emission from a Rose Bengal sample was used in order to align the optical components and maximise the detected IR phosphorescence signal. Confirmation that the detected signal was due to the phosphorescence of singlet oxygen was achieved by collecting the entire spectrum over the range 1200–1350 nm.

Addition of tetruryl alcohol (FFA), a known singlet oxygen quencher,^{35,36} or degassing the sample by multiple freeze–pump–thaw cycles at *ca.* 10^{-5} mbar using a Schlenk line to remove the dissolved oxygen, resulted in elimination of the detected signal.

The analysis of the results requires the calculation of the absorbed incident light, I_{abs} . This parameter was determined using eqn (1) in which I_{λ} is the corrected PoliLight intensity at the wavelength λ and abs_{λ} is the absorbance of the photosensitiser both at the wavelength λ .

$$I_{\text{abs}} = \sum_{\lambda} (1 - 10^{-\text{abs}_{\lambda}}) I_{\lambda} \quad (1)$$

The singlet oxygen quantum yield (Φ_{Δ}) was determined employing the reference sensitiser, Rose Bengal (RB) that has been used previously with a $\Phi_{\Delta} = 0.79$ in methanol.^{4,21,37} The phosphorescence intensity could be monitored at the λ_{max} since no spectral shift of the singlet oxygen phosphorescence spectrum was observed in the different solvents.³⁸ The singlet oxygen quantum yields are determined using a variation of the method used by Tanielian and Heinrich²¹ and using eqn (2)

$$\Phi_{\Delta_s} = \frac{I_r I_{\Delta_r} \tau_r}{I_s I_{\Delta_s} \tau_s} \Phi_{\Delta_r} \quad (2)$$

where I_s and I_r represent the absorbed incident light, and I_{Δ_s} and I_{Δ_r} are the singlet oxygen emission intensities at 1278 nm, for the sample and reference respectively. τ_r and τ_s are the singlet oxygen phosphorescence lifetimes in the reference and the sample solvents and Φ_{Δ_r} is the singlet oxygen quantum yield of the reference compound. Φ_{Δ} measurements were performed in triplicate with a maximum deviation of 10%. Another possible source of error is in the reliability of published singlet oxygen lifetimes used for the calculations.

Results and discussion

Absorption and fluorescence spectra

Steady state UV-visible absorption spectroscopy of the free-base (Fb) porphyrins yielded spectra with the characteristic Soret and Q-band structure that can be explained by the 4-orbital model of Gouterman.³⁹ The porphyrins investigated exhibit different substituents for the pyrrole *exo*-hydrogens of the porphine backbone. Such substitutions are known not to significantly perturb the optical spectra.⁴⁰ The absence of dimers or higher aggregates in the Φ_{Δ} determination experiments was confirmed as the absorption exhibited no variation in spectral shape or position over the sample concentration range investigated.

Porphyrins are able to act as acids or bases⁴¹ that lead to characteristic changes in the absorption spectra consistent with the predictions of the 4-orbital model. The decrease in the observed number of Q-bands upon protonation of the macrocyclic core arises from the increase in symmetry of the porphyrin ring that leads to the degeneracy of the S_1 and S_2 levels.⁴⁰ On the other hand the absorption spectrum of the di-anion form of BOPP observed at high pH values is identical to that of the free-base form. A significant reduction in the fluorescence emission intensity is observed from the di-cation form of BOPP in all the solvents investigated. Although the acid–base properties of BOPP have been reported previously,⁴² these investigations were limited to the pH range between 5 and 7.4 in phosphate buffered solutions

and the reduction in fluorescence for the BOPP di-cation was not reported. A similar decrease in the fluorescence intensity is not observed for the di-cation forms of the HpD and Hp9 porphyrins. It should be noted that BOPP has been suggested for use as both a phototherapeutic agent and in neutron capture therapy^{33,42} while HpD is a mixture of porphyrin monomers and oligomers prepared from Hp9.³²

The metallated forms of porphyrins are common in Nature, and play particularly important roles in electron transfer processes.⁴⁰ The electronic spectra of metalloporphyrins have been classified into three classes; *normal*, *hypo* and *hyper*, dependent on the nature of the intercalating metal.⁴⁰ Insertion of Zn^{2+} into the macrocyclic core results in a similar change in the absorption and fluorescence spectra as observed with the Hp9 and HpD samples in an acidic environment due to a similar change in symmetry designation of the macrocycle. Insertion of Zn^{2+} into the macrocycle is known to produce *normal* spectra according to the definition given by Gouterman.⁴⁰

The series of transition metals used in this work were chosen such that there was a systematic increase in the respective number of electrons in the d-orbital. Of the six metals investigated, only Cu and Zn were able to coordinate to all three porphyrins. Metallation of the BOPP macrocycle was achieved by the majority of the metals. Monitoring the change in the absorption spectra associated with the alteration in symmetry of the macrocycle that occurs upon metallation of the porphyrin provides a method of confirming that metallation has occurred. The absorption spectra of the metallated porphyrins are presented in Fig. 2 and 3. Addition of either Fe^{2+} or Ni^{2+} to solutions of the porphyrins resulted in no observable change to the absorption spectra and thus these ions were assumed not to coordinate to the macrocycle.

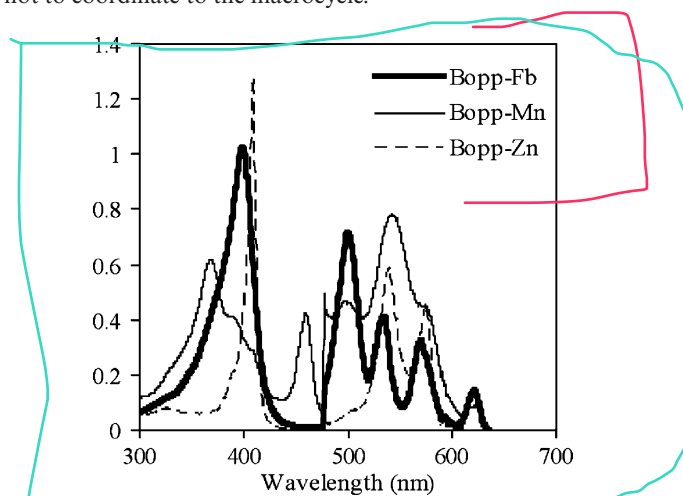


Fig. 2 Absorption spectra of BOPP in methanol before and after the inclusion of Mn^{2+} and Zn^{2+} into the macrocyclic core of the porphyrin molecule. The Q-band region of the spectrum has been enhanced by a factor of 10 for clarity.

The absorption spectrum of BOPP–Mn was significantly different to that observed with insertion of the other metals. Similar spectra have been noted previously for other porphyrins upon insertion of Mn^{2+} .⁴³ The extra band that is observed in Fig. 2 for the BOPP–Mn complex is ascribed to a ring-to-metal charge transfer transition between the $a_{1u}(\pi)$, $a_{2u}(\pi)$ (ring) \rightarrow $e_g(d_{\pi})$ (metal) states.⁴⁰ Therefore, BOPP–Mn can be designated as a d-type *hyper*

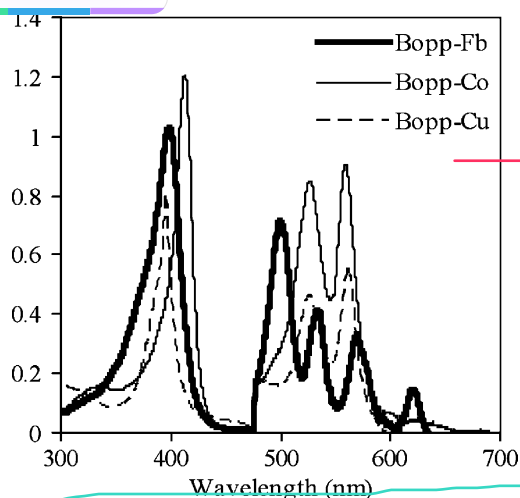


Fig. 3 Absorption spectra of BOPP in methanol before and after the addition of **Co and Cu** into the macrocyclic core of the porphyrin molecule. The Q-band region of the spectrum has been enhanced by a factor of 10 for clarity.

porphyrin. For such an assignment, the transition metal must firstly have a configuration of d^m where $1 \leq m \leq 6$ with one or more vacancies in the $e_g(d\pi)$ orbital and must also exhibit a relatively low oxidation state.⁴⁰ The Mn cation fulfils these criteria. The insertion of the Co and Cu metal ions into the macrocycle results in *hypso*-type spectra. Such a designation is made if the energy of the metal d-electrons decreases with increasing electron count leading to a subsequent increase in the energy gap between the porphyrin LUMO and the metal valence orbitals. This is exhibited in the absorption spectra of the Q-band region becoming less blue shifted as the d-electron count increases.⁴⁴ This is clearly the case as shown in Fig. 3.

The ability of BOPP to accommodate the majority of the metals investigated suggests that the “pocket” available to the metal in BOPP is more accessible than those offered by Hp9 and HpD. Investigating the kinetics of metallation with Zn^{2+} showed that complete metallation was noticeably faster for the BOPP samples compared to Hp9 and HpD after an excess of metal salt was added. Coordination of metals into BOPP occurred over a period of approximately 15 min. The Hp9 and HpD samples exhibited much slower metallation rates with complete complexation occurring over two to three hours. Fig. 4 shows a log-log plot of the change in absorbance at 498 nm *versus* time after the addition of the metal salt to a Fb sample.

Previous studies have shown that co-addition of a large metal ion improves the metallation kinetics of porphyrins.⁴⁵ The large metal ion is thought to act as a catalyst for the insertion of a medium sized metal. The large metal ion is too large to fit into the nucleus of the porphyrin so loosely coordinates with the nitrogens in the macrocyclic core in a “sitting-atop” orientation. Due to the weak nature of the coordination, this association occurs very rapidly. The coordination favourably deforms the ring from planarity to increase the size of the macrocycle and facilitate insertion of the medium sized metal from the alternate face.⁴⁶ Theoretical investigations also confirm a deviation from planarity of the macrocycle during the course of a metallation event.⁴⁷

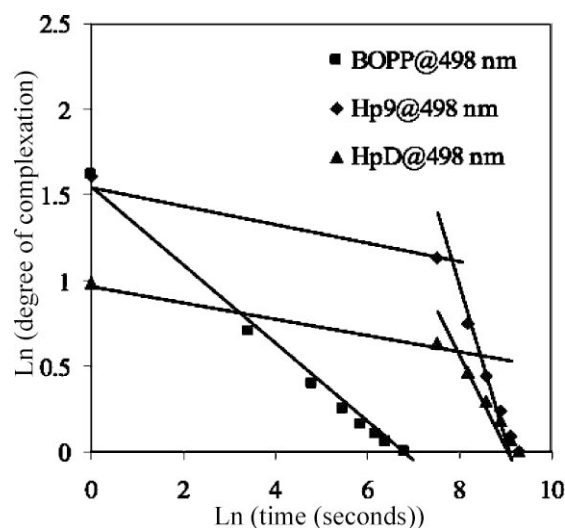


Fig. 4 Log-log plot of time (s) *versus* degree of complexation of Zn^{2+} at 498 nm for BOPP, Hp9 and HpD samples of the same concentration (10^{-4} M). The degree of complexation is defined as: (absorbance at 498 nm at time t)/(absorbance at 498 nm at time infinity).

The bulky peripheral substituents of porphyrins are known to be a factor in influencing the non-planarity of the macrocycles.⁴⁸ The large *closo*-carborane pendant cages in BOPP might similarly be expected to lead to a disruption in the planarity of the ring, and therefore facilitate intercalation of the metal ion. This accounts for the observation that the majority of the transition metals investigated were able to coordinate with BOPP whilst only two of the metal ions, Cu^{2+} and Zn^{2+} , proposed to be close to an optimal size to fit into the porphyrin macrocycle, were able to coordinate into the Hp9 and HpD cores.

Coordination of a metal to a concentrated sample of Hp9 in methanol can be used to illustrate that it is able to form dimers at concentrations considerably lower than observed for the other two porphyrins. It is well known that some porphyrins are able to form dimers with the planar porphyrin-Fb monomers existing in a slightly offset face-to-face arrangement.⁴⁹ The bulky peripheral substituents of BOPP might be expected to hinder such interactions. The addition of either the Zn or Cu salt to a reasonably concentrated (6×10^{-5} M) sample of Hp9 led to an immediate reversion of the absorption spectrum to the four Q-bands typical of the monomer Fb form indicating dimer formation was disrupted (see Fig. 5). The disaggregation is explained by the metal ion attaching loosely to the macrocyclic core that serves to disrupt the planar nature of the ring. The subsequent intercalation of the second metal occurs on a much longer timescale (several hours) as shown in Fig. 4. For BOPP, however, only one rate is evident during the relatively rapid metallation process.

The fluorescence spectra obtained from the Fb and Zn forms of the porphyrins adhered to the general behaviour expected from the 4-orbital model. The fluorescence, while low, has been proposed to be sufficient in aiding diagnosis of cancer when used as photosensitisers in PDT.^{50,51} The fluorescence emission from the porphyrins coordinated to the majority of the transition metals, as well as of the BOPP di-cation, was negligible. While enhanced inter-system crossing to the triplet state might be expected following metallation of the porphyrins due to the heavy-atom effect,⁵² this may not necessarily lead to higher singlet

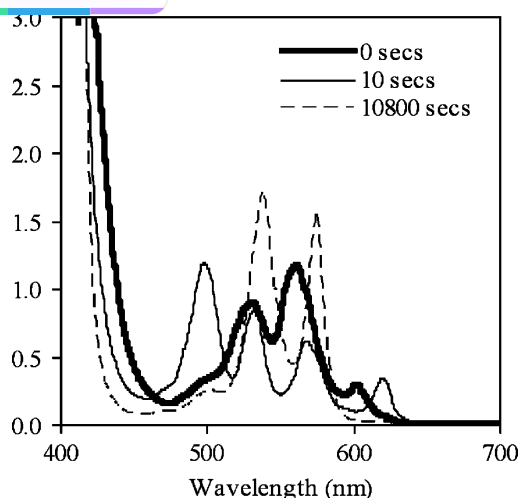


Fig. 5 Absorption spectra showing disaggregation of Hp9-Fb in methanol upon addition of a Zn salt. Concentration of the sample is 6×10^{-5} M.

oxygen quantum yields if the triplet state lifetime is shortened. The fluorescence yields of the di-cation forms of Hp9 and HpD are only slightly lower than those of the corresponding Fb forms.

Singlet oxygen quantum yield determination

The NIR emission resulting from the deactivation of singlet oxygen is known to be absorbed by the terminal bonds of the solvents according to the respective energies of the highest fundamental vibration of that bond.⁵³ Therefore, solvents containing O–H bonds are able to quench singlet oxygen phosphorescence to a greater degree than solvents containing heavier atoms in the terminal bonds.⁵⁴ The $^1\Delta_g \rightarrow ^3\Sigma_g^-$ emission maximum has been reported to be 1270 nm in solution.^{24,55} In the current investigations, the emission spectrum was slightly red-shifted to be centred at 1278 nm. It should be noted that the spectra obtained were uncorrected for the spectral response of the spectrograph/detector combination but the observed phosphorescence maximum is identical to that reported in a previous study where the same type of germanium detector was used.⁵⁶

A concentration dependence on the singlet oxygen quantum yield for the different photosensitisers was investigated. The sum of the corrected intensity of the absorbed incident light (I_{abs}) and the detected phosphorescence intensity at 1278 nm (I_{Δ}) is expected to follow a linear relationship at sufficiently low concentrations and this is evident in Fig. 6 for BOPP-Fb in acetone. The deviation from linearity in Fig. 6 at higher I_{abs} values is associated with using high concentrations and a filter combination allowing excitation of the porphyrin Soret absorption band. For the values of Φ_{Δ} reported in this work only data in the linear region were used. The singlet oxygen quantum yields were calculated using eqn (2) using RB in methanol as the reference. The values of Φ_{Δ} are presented in Table 1.

Porphyrins are generally known to produce impressively high yields of $^1\text{O}_2$.⁵⁷ This is confirmed in the current study. Similar Φ_{Δ} values are obtained for the Fb forms of Hp9 and HpD; whilst those of BOPP are slightly lower in the respective solvents. Previously calculated values for HpD-Fb in methanol of $\Phi_{\Delta} = 0.64$,⁵⁸ Hp9-Fb in methanol of $\Phi_{\Delta} = 0.74$ ³⁷ and RB in ethanol of $\Phi_{\Delta} = 0.86$ ^{34,59}

Table 1 Singlet oxygen quantum yields of the Fb, di-cation and Zn metallated forms of the porphyrins. Literature values for the singlet oxygen lifetimes (τ_{Δ}) required in eqn (2) are also shown

| | Methanol | Ethanol | Acetone | Acetonitrile |
|--------------------------------|-------------------|---------|---------|--------------|
| $\tau_{\Delta}/\mu\text{s}^a$ | 10.0 | 14.5 | 55.4 | 83.7 |
| Φ_{Δ} Rose Bengal | 0.79 ^b | 0.88 | 0.70 | 0.65 |
| Φ_{Δ} BOPP | 0.58 | 0.67 | 0.58 | 0.44 |
| Φ_{Δ} BOPP-di-cation | 0.00 | 0.00 | 0.02 | 0.01 |
| Φ_{Δ} BOPP-Zn | 0.45 | 0.56 | 0.52 | 0.33 |
| Φ_{Δ} Hp9 | 0.68 | 0.85 | 0.69 | 0.51 |
| Φ_{Δ} Hp9-di-cation | 0.69 | 0.83 | 0.60 | 0.52 |
| Φ_{Δ} Hp9-Zn | 0.42 | 0.50 | 0.49 | 0.27 |
| Φ_{Δ} HpD | 0.64 | 0.85 | 0.60 | 0.52 |
| Φ_{Δ} HpD-di-cation | 0.63 | 0.78 | 0.57 | 0.49 |
| Φ_{Δ} HpD-Zn | 0.56 | 0.73 | 0.53 | 0.27 |

^a Ref. 60. ^b Ref. 4, 21 and 37.

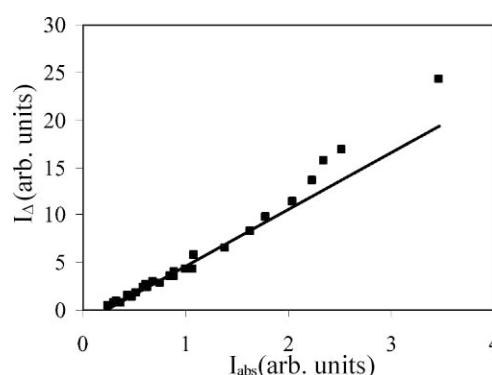


Fig. 6 Phosphorescence intensity versus the integrated light absorption for BOPP-Fb in acetone. I_{abs} values were calculated using eqn (2). The phosphorescence intensity was monitored at 1278 nm.

are in excellent agreement with the values of $\Phi_{\Delta} = 0.64$, $\Phi_{\Delta} = 0.68$ and $\Phi_{\Delta} = 0.89$ respectively obtained in the current study.

Negligible singlet oxygen production from the BOPP-di-cation suggests that efficient internal conversion competes with triplet state formation in this system. The calculated quantum yields of the di-cation forms of both Hp9 and HpD are almost identical to those obtained from the Fb forms in the corresponding solvent. Such a direct comparison is valid since the solubility of oxygen has been shown not to change with pH.³⁴ While the small addition of aqueous acid to protonate the porphyrin can potentially reduce the lifetime of singlet oxygen (due to the presence of water), control experiments with similar additions of water did not significantly affect singlet oxygen yields.

Porphyrins can contain 2 core hydrogens with minimal strain exerted on the ring. The addition of the two extra protons to the macrocyclic core that is observed in the porphyrin di-cation, results in an excessive crowding in the core.⁶¹ Easing of this steric strain is achieved by deformation of the porphyrin ring from a planar configuration. Porphyrins are known to take up one of five non-planar orientations.⁶² Di-cation porphyrins typically take up a saddle conformation.⁶³ As observed from the steady-state investigation of the insertion of transition metals into the macrocycle of BOPP, the non-planarity is suggested to be augmented by the large peripherally substituted *closo*-carborane pendant groups. The non-planarity leads to an almost complete quenching of both the fluorescence and the singlet

oxygen quantum yields. Quenching of the fluorescence in sterically crowded porphyrins has been observed,^{64,65} although the decrease in Φ_A has not been reported previously. The effect of the distortion of the macrocycle on excited electronic singlet and triplet states has been considered.⁶⁶ In the cases of Hp9 and HpD, the smaller peripheral substituents which would not accentuate the ring non-planarity as significantly as is proposed for the BOPP porphyrin, results in no significant quenching of the fluorescence and singlet oxygen phosphorescence.

The presence of a metal is known to often lead to an enhancement in the ISC pathway in an excited molecule due the "heavy atom effect".⁶⁷ The magnitude of the effect has theoretical grounding based on Fermi's golden rule indicating that the rate constant for ISC is proportional to the square of the atomic number of the heavy atom.⁶⁸ The calculated values of the singlet oxygen quantum yield for the Zn porphyrins are presented in Table 1. Metallation of the porphyrins with a Zn ion led to a decrease in the singlet oxygen quantum yield compared to that observed from the Fb form in the corresponding solvent. This can be attributed to either enhanced internal conversion or an increase in the rate of back ISC to the ground state.⁴⁰ It seems unlikely that the triplet state lifetimes of the metallated porphyrins would be reduced to such an extent that diffusional interactions with oxygen would not take place and it seems most likely that enhanced internal conversion from the singlet state is responsible for lower triplet yields and the observed decreased Φ_A values.

Although the general trend of Φ_A values is followed for the Zn porphyrins in the different solvents, the results in acetonitrile differ to a greater degree than expected when compared to the RB samples. Acetonitrile solvent molecules are known to coordinate axially with the zinc centre in investigations on other porphyrins.^{69,70} Such binding is known to influence the yield and lifetime of the triplet state. It has also been reported that coordination of axial ligands to a metalloporphyrin can lead to a disruption in the planarity of the ring.⁷¹

As mentioned in the discussion of the BOPP di-cation, a significant influence on the electronic properties of the photosensitiser is known to arise from the deviations from planarity induced to the tetrapyrrolic ring.^{64,72} Metallation of porphyrins is known to be a factor in altering the planarity of porphyrins.^{73–75} Spectroscopic^{76,77} as well as molecular modelling^{74,75,78} coupled with the normal-coordinate structural decomposition method^{62,78,79} have been shown to be essential tools in investigating the non-planarity of metallated porphyrins. The coordination of transition metals into the macrocyclic core is known to perturb the ring π -electron system and introduce several low lying charge transfer (CT) states.⁸⁰ Such states may be metal–ligand, ligand–metal or metal–metal states.⁸¹ Previous investigations into Zn porphyrins have determined that the Zn^{2+} ion is conducive to maintaining the planar nature of the macrocycle.⁴⁸ Therefore, the perturbation induced by metallation to the macrocyclic ring by the diamagnetic Zn^{2+} ion is small and the excited states may be regarded as normal ($\pi-\pi^*$) singlet and triplet states. As mentioned above, a markedly lower value of Φ_A is obtained for the Zn porphyrin in acetonitrile samples. The uneven axial coordination of an acetonitrile solvent molecule to the Zn metal would increase the non-planarity of the ring^{70,71} and account for the lower values of Φ_A obtained.

As mentioned above, under the conditions used, only Cu^{2+} and Zn^{2+} ions were able to complex to all three porphyrins studied,

while Mn^{2+} and Co^{2+} could also be incorporated into the BOPP macrocycle. There was no detectable singlet oxygen formation observed in methanol solutions of the Cu^{2+} complexes of Hp9 and HpD and for the Co^{2+} and Cu^{2+} complexes of BOPP. The Mn^{2+} complex of BOPP exhibited a much reduced value for Φ_A of 0.04 compared to the free-base form. The insertion of Mn to BOPP results in a d-type *hyper* absorption spectrum. Therefore, the ligand to metal charge transfer that occurs between the porphyrin orbitals and the vacancies in the metal $e_g(d_\pi)$ orbitals might be expected to lead to the significant quenching in both the singlet oxygen production as well as fluorescence. For the other transition metals, the mixing of nd_π (metal) with the $e_g(\pi^*)$ (porphyrin) orbitals give rise to a greater spin–orbital coupling that in turn leads to an increase in the decay rates of both radiative and non-radiative processes between the singlet and triplet states.⁴⁰ The resulting shortened excited state lifetimes would decrease the likelihood for singlet oxygen formation.⁸²

Conclusions

Singlet oxygen formation quantum yields have been determined for different forms of three porphyrins in several solvents using the method of direct detection of the $^1\Delta_g$ phosphorescence. The singlet oxygen quantum yields of the Fb forms of the three porphyrins and the reference compound RB follow a similar trend in the different solvents studied. Higher values of Φ_A were obtained from the free-base forms of Hp9 and HpD compared to those of BOPP in the respective solvents. No change in Φ_A for the di-cation forms of Hp9 and HpD was observed compared to the values obtained from the Fb forms. However, an almost complete reduction of singlet oxygen production as well as the fluorescence is noted for the BOPP di-cation. This unusual observation is proposed to result from the increased non-planarity of the macrocycle arising from the steric crowding caused by the four hydrogens now in the core. Although such steric crowding would also be expected for the di-cation forms of Hp9 and HpD, the non-planarity is augmented in BOPP by the bulky nature of the peripheral substituents.

The effects of incorporating a number of first row transition metals were investigated in this study. BOPP allowed a greater number of the metals to coordinate to the macrocyclic core, arising from a favourable disruption of planarity of the ring exerted by the large *closo*-carborane cages. A complete reduction of Φ_A was observed following insertion of the majority of the transition metals able to coordinate to the porphyrins. Coordination of Zn^{2+} to the porphyrins led to a decrease of Φ_A by a factor of 0.8 for BOPP and HpD and 0.6 for Hp9 compared to the Fb forms. It is proposed that enhancement of competing non-radiative processes accounts for this observation.

The investigations reported here indicate that the optimal singlet oxygen quantum yields for all three porphyrins are obtained for the Fb forms with equally high yields obtained from the di-cation forms of Hp9 and HpD. The high values of Φ_A obtained confirm that each free-base porphyrin would be viable candidates as photosensitisers in PDT. On the basis of singlet oxygen production, metallated porphyrins are less suitable for phototherapy applications. The facile incorporation of zinc ions into the porphyrin macrocycle suggests the possibility that adventitious zinc ions in the body may be included into free-base porphyrins used for phototherapy, thus diminishing their

effectiveness. The localisation behaviour of zinc porphyrins within the cell and associated phototoxicity might possibly compensate to some extent for the reduced singlet oxygen yields. Future fluorescence imaging studies of these porphyrins in cells should assist in resolving such possibilities.

Acknowledgements

We wish to thank Stan Stylli of the Department of Surgery, Royal Melbourne Hospital for the provision of the BOPP sample.

References

- 1 J. S. Valentine, D. L. Wertz, T. J. Lyons, L.-L. Liou, J. J. Goto and E. B. Gralla, *Curr. Opin. Chem. Biol.*, 1998, **2**, 253.
- 2 R. S. Mulliken, *Phys. Rev.*, 1928, **32**, 186.
- 3 J. R. Kanofsky, Assay for singlet oxygen generation by peroxidases using 1270 nm chemiluminescence, in *Methods of Enzymology*, ed. L. Packer and H. Sies, Academic Press, New York, 2000, p. 59.
- 4 F. Wilkinson, W. P. Helman and A. B. Ross, *J. Chem. Ref. Data*, 1995, **24**, 663.
- 5 G. Herzberg, *Spectra of Diatomic Molecules*, Van Nostrand Reinhold, New York, 1950.
- 6 R. Schmidt and M. Bodesheim, *J. Phys. Chem.*, 1995, **99**, 15919.
- 7 H. Kautsky, *Trans. Faraday Soc.*, 1939, **35**, 216.
- 8 A. M. Held, D. J. Halko and J. K. Hurst, *J. Am. Chem. Soc.*, 1978, **100**, 5732.
- 9 A. P. Napartovich, A. A. Deryugin and I. V. Kochetov, *J. Phys. D: Appl. Phys.*, 2001, **34**, 1827.
- 10 C. Schweitzer and R. Schmidt, *Chem. Rev.*, 2003, **103**, 1685.
- 11 J. R. Hurst, J. D. McDonald and G. B. Schuster, *J. Am. Chem. Soc.*, 1982, **104**, 2065.
- 12 J. G. Parker and W. G. Stanbro, *J. Am. Chem. Soc.*, 1982, **104**, 2067.
- 13 M. A. J. Rodgers and P. T. Snowden, *J. Am. Chem. Soc.*, 1982, **104**, 5541.
- 14 F. Prat, C. Marti, S. Nonell, X. Zhang, C. S. Foote, R. G. Moreno, J. L. Bourelle and J. Font, *Phys. Chem. Chem. Phys.*, 2001, **3**, 1638.
- 15 R. W. Redmond, *Photochem. Photobiol.*, 1991, **54**, 547.
- 16 R. Schmidt, C. Tanielian, R. Dunsbach and C. Wolff, *J. Photochem. Photobiol., A*, 1994, **79**, 11.
- 17 G. Rossbrich, N. A. Garcia and S. E. Braslavsky, *J. Photochem.*, 1985, **31**, 37.
- 18 K. Fuke, M. Ueda and M. Itoh, *Chem. Phys. Lett.*, 1980, **76**, 372.
- 19 R. W. Redmond and S. E. Braslavsky, *Chem. Phys. Lett.*, 1988, **148**, 523.
- 20 K. Gollnick, T. Franken, G. Schade and G. Dorhofer, *Ann. N. Y. Acad. Sci.*, 1970, **171**, 89.
- 21 C. Tanielian and G. Heinrich, *Photochem. Photobiol.*, 1995, **61**, 131.
- 22 C. Marti, O. C. Jurgens, M. Casals and S. Nonell, *J. Photochem. Photobiol., A*, 1996, **97**, 11.
- 23 V. Gottfried, D. Peled, J. W. Winkerman and S. Kimel, *Photochem. Photobiol.*, 1988, **48**, 157.
- 24 A. A. J. Krasnovsky, *Photochem. Photobiol.*, 1979, **29**, 29.
- 25 P. Bilski, B. M. Kukielczak and C. F. Chignell, *Photochem. Photobiol.*, 1998, **68**, 675.
- 26 Liquid Nitrogen cooled Germanium Detector, 403 L, *Applied Detector Corporation*, Fresno, California, 1994.
- 27 NIR Photomultiplier Tubes R5509-43/R5509-72, *Hamamatsu Photonics K.K.*, 2003.
- 28 NIR-PMT Module, *Hamamatsu Photonics K.K.*, 2003.
- 29 A. P. Castano, *Photodiagn. Photodyn. Ther.*, 2005, **2**, 1.
- 30 A. P. Castano, *Photodiagn. Photodyn. Ther.*, 2005, **2**, 91.
- 31 A. P. Castano, T. N. Demidova and M. R. Hamblin, *Photodiagn. Photodyn. Ther.*, 2004, **1**, 279.
- 32 B. W. Henderson and T. J. Dougherty, *Photodynamic Therapy: Basic Principles and Clinical Applications*, Marcel Dekker, New York, 1992.
- 33 S. B. Kahl and M.-S. Koo, *J. Chem. Soc., Chem. Commun.*, 1990, **24**, 1769.
- 34 R. Bonneau, R. Pottier, O. Bagno and J. Joussot-Dubien, *Photochem. Photobiol.*, 1975, **21**, 159.
- 35 P. Murasecco, E. Oliveros, A. M. Braun and P. Monnier, *Photobiophys.*, 1985, **9**, 193.
- 36 W. R. Haag, J. Hoigne, E. Gassman and A. M. Braun, *Chemosphere*, 1984, **13**, 631.
- 37 C. Tanielian, C. Wolff and M. Esch, *J. Phys. Chem.*, 1996, **100**, 6555.
- 38 P. Bilski, R. N. Holt and C. F. Chignell, *J. Photochem. Photobiol., A*, 1997, **109**, 243.
- 39 M. Gouterman, G. H. Wagniere and L. C. Snyder, *J. Mol. Spectrosc.*, 1963, **11**, 108.
- 40 M. Gouterman, Optical Spectra and Electronic Structure of Porphyrins and Related Rings, in *The Porphyrins*, ed. D. Dolphin, Academic Press, New York, 1978.
- 41 B. Cunderlikova, E. G. Bjorklund, E. O. Pettersen and J. Moan, *Photochem. Photobiol.*, 2001, **74**, 246.
- 42 P. G. Spizzirri, J. S. Hill, S. B. Kahl and K. P. Ghiggino, *Photochem. Photobiol.*, 1996, **64**, 975.
- 43 M. H. Gelb, W. A. J. Toscano and S. G. Sligar, *Proc. Natl. Acad. Sci. USA*, 1982, **79**, 5758.
- 44 K. S. Suslick and R. A. Watson, *New J. Chem.*, 1992, **16**, 633.
- 45 M. Tanaka, *Pure Appl. Chem.*, 1983, **55**, 151.
- 46 J. A. Shellnut, X.-Z. Song, J.-G. Ma, S.-L. Jia, W. Jentzen and C. J. Medforth, *Chem. Soc. Rev.*, 1998, **27**, 31.
- 47 Y. Shen and U. Ryde, *Chem.-Eur. J.*, 2005, **11**, 1549.
- 48 J. A. Shellnut, C. J. Medforth, M. D. Berber, K. M. Barkigia and K. M. Smith, *J. Am. Chem. Soc.*, 1991, **113**, 4077.
- 49 C. A. Hunter and J. K. M. Sanders, *J. Am. Chem. Soc.*, 1990, **112**, 5525.
- 50 M. S. Eljamel, *Tech. Cancer Res. Treat.*, 2003, **2**, 303.
- 51 A. Sieron, A. Kawczyk-Krupka, M. Adamek, W. Cebula, W. Zieleznik, K. Niepsuj, G. Niepsuj, A. Pietrusa, M. Szygula, T. Biniszkiwicz, S. Mazur, J. Malyszek, A. Romanczyk, A. Lewdwon, A. Frankiewicz, A. Zybura, E. Koczy and B. Birkner, *Photodiagn. Photodyn. Ther.*, 2006, **3**, 132.
- 52 T. Medinger and F. Wilkinson, *Trans. Faraday Soc.*, 1965, **61**, 620.
- 53 O. Shimizu, J. Watanabe, K. Imakubo and S. Naito, *J. Phys. Soc. Jpn.*, 1998, **67**, 3664.
- 54 P. R. Ogilby and C. S. Foote, *J. Am. Chem. Soc.*, 1983, **105**, 3423.
- 55 P. B. Merkel and D. R. Kearns, *J. Am. Chem. Soc.*, 1972, **94**, 7244.
- 56 J. M. Wessels, P. Charlesworth and M. A. J. Rodgers, *Photochem. Photobiol.*, 1995, **61**, 350.
- 57 N. J. Turro, *Modern Molecular Photochemistry*, University Science Books, California, 2003.
- 58 C. Tanielian, C. Schweitzer, R. Mechin and C. Wolff, *Free Radical Biol. Med.*, 2002, **30**, 208.
- 59 E. Gandin, Y. Lion and A. Van de Vorst, *Photochem. Photobiol.*, 1983, **37**, 271.
- 60 O. Shimizu, J. Watanabe, K. Imakubo and S. Naito, *Chem. Lett.*, 1999, **67**.
- 61 M. O. Senge, T. P. Forsyth, L. T. Nguyen and K. M. Smith, *Angew. Chem., Int. Ed. Engl.*, 1994, **33**, 2485.
- 62 W. Jentzen, J.-G. Ma and J. A. Shellnut, *Biophys. J.*, 1998, **74**, 753.
- 63 M. O. Senge, *The Porphyrin Handbook*, Academic Press, Boston, 2000.
- 64 C. M. Drain, C. Kirmaier, C. J. Medforth, D. J. Nurco, K. M. Smith and D. Holten, *J. Phys. Chem.*, 1996, **100**, 11984.
- 65 S. Gentemann, C. J. Medforth, T. P. Forsyth, D. J. Nurco, K. M. Smith, J. Fajer and D. Holten, *J. Am. Chem. Soc.*, 1994, **116**, 7363.
- 66 V. I. Gael, V. A. Kuz'mitskii and K. N. Solov'ev, *J. Appl. Spectrosc.*, 2000, **67**, 956.
- 67 A. Weihe, H. Stollberg, S. Runge, A. Paul, M. O. Senge and B. Roder, *J. Porphyrins Phthalocyanines*, 2001, **5**, 853.
- 68 E. Fermi, *Nuclear Physics*, University of Chicago Press, 1950.
- 69 I. Mayer, M. N. Eberlin, D. M. Tomazela, H. E. Toma and K. Araki, *J. Braz. Chem. Soc.*, 2005, **16**, 418.
- 70 Y. Inada, Y. Nakano, M. Inamo, M. Nomura and S. Funahashi, *Inorg. Chem.*, 2000, **39**, 4793.
- 71 K. S. Suslick, N. A. Rakow, M. E. Kosal and J.-H. Chou, *J. Porphyrins Phthalocyanines*, 2000, **4**, 407.
- 72 C. J. Medforth, M. O. Senge, K. M. Smith, L. P. Sparks and J. A. Shellnut, *J. Am. Chem. Soc.*, 1992, **114**, 9859.
- 73 D. J. Nurco, C. J. Medforth, T. P. Forsyth, M. M. Olmstead and K. M. Smith, *J. Am. Chem. Soc.*, 1996, **118**, 10918.
- 74 X.-Z. Song, W. Jentzen, S.-L. Jia, L. Jaquinod, D. J. Nurco, C. J. Medforth, K. M. Smith and J. A. Shellnut, *J. Am. Chem. Soc.*, 1996, **118**, 12975.
- 75 L. D. Sparks, C. J. Medforth, M.-S. Park, J. R. Chamberlain, M. R. Ondrias, M. O. Senge, K. M. Smith and J. A. Shellnut, *J. Am. Chem. Soc.*, 1993, **115**, 581.

- 76 C. J. Medforth, J. D. Hobbs, M. R. Rodriguez, R. J. Abraham, K. M. Smith and J. A. Shelnutt, *Inorg. Chem.*, 1995, **34**, 1333.
- 77 M. S. Somma, C. J. Medforth, N. Y. Nelson, M. M. Olmstead, R. G. Khoury and K. M. Smith, *Chem. Commun.*, 1999, 1221.
- 78 W. Jentzen, M. C. Simpson, J. D. Hobbs, X. Song, T. Ema, N. Y. Nelson, C. J. Medforth, K. M. Smith, M. Veyrat, M. Mazzanti, R. Ramasseul, J.-C. Marchon, T. Takeuchi, W. A. Goddard III and J. A. Shelnutt, *J. Am. Chem. Soc.*, 1995, **117**, 11085.
- 79 W. Jentzen, X.-Z. Song and J. A. Shelnutt, *J. Phys. Chem. B*, 1997, **101**, 1684.
- 80 A. V. Zamyatin, A. V. Gusev and M. A. J. Rodgers, *J. Am. Chem. Soc.*, 2004, **126**, 15934.
- 81 K. Kandasamy, S. J. Shetty, P. N. Puntambekar, T. S. Srivastava, T. Kundu and B. P. Singh, *J. Porphyrins Phthalocyanines*, 1999, **3**, 81.
- 82 A. Antipas, J. W. Buchler, M. Gouterman and P. D. Smith, *J. Am. Chem. Soc.*, 1978, **100**, 3015.